Specific and differential binding of *N*-acetylgalactosamine glycopolymers to the human Macrophage Galactose Lectin and Asialoglycoprotein Receptor

Joji Tanaka,[a] Anne S. Gleinich,[b] Qiang Zhang,[a†] Richard Whitfield,[a] Kristian Kempe,[c,a] David M. Haddleton,[a,c] Thomas P. Davis, [c,a] Sébastien Perrier,[a,c] Daniel A. Mitchell,[b] and Paul Wilson*[a,c]*

[a]*Chemistry Department, University of Warwick, Library Road, CV4 7AL Coventry, United Kingdom.*

[b]*Clinical Sciences Research Institute, Warwick Medical School, University of Warwick, CV2 2DX.*

[c]*ARC Centre of Excellence in Convergent Bio-Nano Science and Technology, Monash Institute of Pharmaceutical Sciences, Monash University (Parkville Campus), 399 Royal Parade, Parkville, Victoria 3152, Australia.*

KEYWORDS Glycopolymer, N-acetylgalactosamine, Macrophage Galactose Lectin, Asialoglycoprotein Receptor, Surface Plasmon Resonance, Atom Transfer Radical Polymerization

ABSTRACT

A range of glycopolymers comprised of *N*-acetylgalactosamine were prepared via sequential Cu(I)-mediated polymerization and alkyne-azide click (CuAAC). The resulting polymers were shown, via multichannel surface plasmon resonance, to interact specifically with human Macrophage Galactose Lectin (MGL; CD301) with high affinity (K_D = 1.11 μM), but did not bind to the mannose/fucose selective human lectin Dendritic Cell-Specific Intercellular adhesion molecule-3-Grabbing Non-integrin (DC-SIGN; CD209). The effect of sugar ligand valency on the binding (so-called 'glycoside cluster effect') of poly(*N*-acetylgalactosamine) to MGL was investigated by varying first the polymer chain length (DP: 100, 64, 40, 23, 12) and then the architecture (4- and 8-arm star glycopolymers). The chain length did not have a significant effect on the binding to MGL (K_D = 0.17 μM – 0.52 μM), however, when compared to a hepatic C-type lectin of a similar monosaccharide specificity, the asialoglycoprotein Receptor (ASGPR), the binding affinity was more noticeably affected (K_D = 0.37 μM – 6.65 μM). These data suggest that known differences in the specific configuration/orientation of the carbohydrate recognition domains of MGL and ASGPR are responsible for the differences in binding observed between the different polymers of varied chain length and architecture. In the future this model has the potential to be employed for the development of tissue selective delivery systems.

INTRODUCTION

Carbohydrate recognition controls many biological processes and is mediated through carbohydrate binding proteins termed lectins.[1] One of the most important classes of human lectins is the C-type lectin class (CTLs),[2–6] and these proteins mediate selective and specific carbohydrate recognition and subsequently drive important functions such as endocytosis.[7] A number of major

C-type lectins are expressed on the surfaces of key immune cells such as macrophages and dendritic cells and have been identified as a potential platform for targeted drug delivery and synthetic vaccination.[8,9] In general all CTLs share high sequence homology and tertiary structure, but the carbohydrate specificity can be generalized into two broad groups by tripeptide motifs in the Carbohydrate Recognition Domain (CRD) that engages calcium chelation and H-bonding with the C3 and C4 hydroxyl groups of the target carbohydrate subcomponent. CTLs such as DC-SIGN and Macrophage Mannose Receptor (MR; CD206) that contain the 'Glu-Pro-Asn' (EPN) motif in the CRD prefer to bind pyranose units with C3/C4 hydroxyls at equatorial/equatorial positions; these include mannose, L-fucose, and *N*-acetylglucosamine (GlcNAc).[10] Physiologically, these mannose-selective CTLs are generally credited as pathogen pattern recognition receptors.[11] In contrast to the several members of EPN type CTLs in humans, there are a small set of CTLs with the 'Gln-Pro-Asp' (QPD) motif in the CRD, and they have preferential binding to galactose-based sugars with the C3/C4 pyranosyl hydroxyls at an equatorial/axial position.[12] For the two major galactose-specific CTLs in the human body, ASGPR and MGL, where the structure and function are not fully understood, there have been no direct comparisons between their binding activities to synthetic ligands. ASGPR is a hepatic CTL largely expressed on sinusoidal face of hepatocyte surfaces, and is responsible for vascular homeostatic regulations[13] mediated by recognition of terminal galactose/GalNAc residues found on senescent de-sialylated glycan clusters found on circulating glycoproteins and platelets.[14] In contrast, MGL is an immunological CTL, expressed on the surface of macrophages and dendritic cells, implicated in stimulating T-cell signaling.[3]

Glycopolymers that interact with biological systems possess considerable potential as novel therapeutics and molecular probes. Recent discoveries have led to complex compositions and architectures, attracting interest in various fields for numerous applications such as biosensors,[15]

drug delivery components[16], cryopreservation, synthetic vaccines[9], immunodulators[8] and cell culture matrices.[17] However, the majority of the literature focuses on interactions with plant derived lectins such as Concanavalin A (ConA),[18] Soybean Agglutinin (SBA),[19] Peanut Agglutinin (PNA)[20] and Helix Pomatia Agglutinin (HPA).[21] In the context of human drug delivery and therapeutic applications, investigating human immunological C-type lectins such as MR, MGL and DC-SIGN is of much higher importance and relevance.

Historically, the synthesis of well-defined glycopolymers has been a challenge, due to the need for complex multistep syntheses. Recently, however, this has been alleviated by the development of methods whereby glycopolymers can be synthesized by direct polymerization of glycomonomers. For example, Davis et al. exploited chemoenzymatic reactions to synthesize (meth)acrylate[22] and vinyl-ester[23] based glycomonomers which were subsequently polymerized by RAFT using dithiocarbonate and xanthate chain transfer agents respectively. Cameron et al. polymerized α-GalNAc functionalized acrylamide by RAFT as a Tn-antigen mimic and coated gold nanoparticles as potential candidates for synthetic, carbohydrate-based anti-cancer vaccines.[24] Haddleton and coworkers, reported sequence controlled glycopolymers synthesized by single electron transfer living radical polymerization (SET-LRP) from a library of glycomonomers.[25] Binding studies with DC-SIGN[26] and its competitive inhibition of the attachment of HIV glycoprotein gp120 was also reported. Finally, De Coen and coworkers used acetylated mannose to prepared a mannose-arcylamide monomer in a single step.[27]

Post-polymerization modification of functional polymer scaffolds is a complimentary, efficient method for generating libraries of glycopolymers, with well-defined scaffolds accessible from commercially available or easily obtainable monomers. Glycidyl (meth)acrylate has been shown to be a versatile monomer, yielding scaffolds capable of undergoing thio-epoxy ring opening in

the presence of thio-sugars,[28] as well as sequential nucleophilic ring opening, by sodium azide, and 'click' with glycosyl alkynes.[29] Activated esters such as pentafluorophenyl and *N*-Hydroxysuccinimide (NHS) ester activated polymers are interesting precursor scaffolds, however they are often hydrolytically unstable and do not necessary yield quantitative conversions.[30] Bertozzi reported a method involving the attachment of non-functionalized sugar to poly(acrylhydrazide) scaffolds via the reducing termini[21], however grafting efficiency is reduced for *N*-acetylated carbohydrates. 'Click' chemistry is an attractive tool for glycopolymer synthesis due to the inherent efficiency and quantitative conversions associated with the reactions. In particular Copper(I)-catalyzed Azide Alkyne Cycloaddition (CuAAC) has been employed over the past decade to generate glycopolymers.[31] Glycosyl azides/alkynes have been efficiently coupled to well-defined alkyne/azide-functional scaffolds which can be synthesized by various radical polymerization protocols including RAFT,[32,33] ATRP[34] and cobalt-mediated CCTP.[35]

Herein we report the synthesis of *N*-acetyl galactosamine glycopolymers and their specific / differential binding to recombinant human MGL and ASPGR lectins. The difference in binding with respect to the degree of polymerization (DP_n) and the molecular architecture is also reported.

EXPERIMENTAL

Materials and methods

N-(ethyl)-2-pyridylmethanimine and trimethylsilyl propargyl methacrylate were synthesised according to previously published work.[36] Copper(I) Bromide (98%, Sigma-Aldrich) was treated with acetic acid and ethanol and dried under vacuum prior to use. Amberlite IR120 (Sigma-Aldrich) was treated with 1M NaOH, de-ionised water and ethanol prior to use. 2-Chloro-1,3-dimethylimdazolinium chloride (DMC) (>97%, Fluka), N-acetyl-D-glucosamine GlcNAc (>98%,

Alfa Aesar), GalNAc (99.6%, Dextra), Triethylamine (TEA) (Fisher scientific, >99%) were used as received. All the other reagents and solvents were obtained from Sigma-Aldrich at the highest purity available and used without any further purification. Dialysis tubing (1KDa MWCO) was supplied by Spectrum Laboratories. Soluble recombinant, tetrameric extracellular domains of DC-SIGN and DC-SIGNR were prepared as previously described.[37] Soluble recombinant Langerin trimeric extracellular domain was obtained from Elicityl SA (Grenoble, France). Soluble recombinant trimeric MGL extracellular domain and trimeric ASGPR H1 extracellular domain proteins were obtained from R&D Systems Inc (Minneapolis, USA). All ^{1}H NMR and ^{13}C NMR spectra were recorded on Bruker HD 300 MHz or 400 MHz spectrometers. The chemical shifts are reported in ppm with respect to the residual peaks of the deutrated solvents used as internal standards and ACDLABS software was used to analyse the data obtained. Infrared absorption spectra were recorded on Bruker VECTOR-22 FT-IR spectrometer using a Golden Gate diamond attenuated total reflection cell and OPUS software was used to analyse the data. Mass spectra were recorded on Bruker Esquire 2000 using ESI. SEC analysis was conducted on Agilent 1260 Infinity Multi-Detector GPC Systems in DMF (1.06 $g\ell^{-1}$ LiBr), calibrated with narrow PMMA standards (200 – 4.7 x 10^5 $g.mol^{-1}$). The GPC data obtained were analysed using Agilent Technologies GPC/SEC software. Melting point was measured using an Optimelt MPA100 system (Stanford Research Systems) and the data was analysed with Meltview v.1.108.

Synthesis

Representative spectra of the sugar azides and glycopolymers synthesized can be found in the supplementary information.

Azido sugars. 2-Chloro-1,3-dimethylimdazolinium chloride (4.6 g, 27.1 mmol, 3 eq) was added to a mixture of H_2O (45 ml), sodium azide (5.9 g, 90.4 mmol, 10 eq), triethylamine (9.2 g, 90.4 mmol, 10 eq) and D-*N*-acetylgalactosamine/ D-*N*-acetylglucosamine (2 g, 9.0 mmol, 1 eq). The reaction was left stirring at 0 ^{0}C for 1 hour and left to stir over night at ambient room temperature. The reaction mixture was concentrated under reduced pressure. Ethanol (100 ml) was added and passed through a short column of Amberlite IR-120. The filtrate was concentrated under reduced pressure. H_2O (10 ml) was added and washed with dichloromethane (3 × 15 ml). The aqueous layer was collected and freeze-dried. The resulting yellow solid was redissolved in methanol (10 ml) and precipitated into dicholoromethane (100 ml) to yield the pure products β-*N*-acetylgalactosamine azide (1.2 g, 4.9 mmol, 54 %) and β-*N*-acetylglucosamine azide (1.0 g, 4.1 mmol, 45 %) that were spectroscopically equivalent to those previously reported in the literature.[38]

General procedure for ATRP of trimethylsilyl propargyl methacrylate (linear); *N*-(ethyl)-2-pyridylmethanimine (34.2 mg, 255.0 μmol, 2 eq), ethyl α-bromoisobutyrate (24.8 mg, 127.0 μmol, 1 eq), trimethylsilyl propargyl methacrylate (2.0 g, 10.2 mmol, 80 eq) and toluene (2 ml) were charged to a dry Schlenk tube. The tube was sealed and subjected to seven freeze-pump-thaw cycles. The resulting de-gassed mixture was transferred via cannula under nitrogen into a second Schlenk tube, previously evacuated and filled with nitrogen, containing Cu(I)Br (18.3 mg, 127.0 μmol, 1 eq) and a magnetic stirrer. The reaction mixture was stirred at 70°C for 6 hours. The conversion was measured by integrating the monomeric OCH_2 (4.74 ppm) and emerging polymeric OCH_2 (4.60 ppm) and comparing it against the vinylic signals (6.16 ppm and 5.58 ppm). The polymerisation was stopped at 70% conversion and terminated by diluting reaction mixture with 10 ml of toluene before bubbling air for 2 hours. The terminated mixture was passed through

a short column of alumina eluting with THF. The solvent was removed under pressure and redissolved in THF (10 ml) prior to precipitation in petroleum ether (200 ml). The precipitate was separated by centrifugation and decanting the solvent to yield poly(trimethylsilyl propargyl methacrylate) (1.1 g) as white solid.

For investigating the effect of chain length ($DP_{n,th}$ = 10, 20, 40, 60, 100) a benzyl functional initiator was employed for more accurate determination of the $DP_{n,NMR}$ using the aromatic protons (7.28-7.38 ppm). The amount of monomer and solvent used was kept constant and the amount of initiator used was in accordance to equation 3. The amount of copper and ligand used was adjusted with the respect to the initiator with absolute ratio of [Initiator] : [Copper] : [Ligand] / 1 : 1 : 2 for each polymerisation.

$$DP_{Theory} = \frac{[monomer]}{[Initiator]} \times Conversion \quad \text{(eq 3)}$$

ATRP of trimethylsilyl propargyl methacrylate (4-arm star); General procedure followed using a pentaerythritol based tetra-initiator.[39] The initiator concentration was calculated according to eq 3 taking each bromine group as an effective initiator to calculate effective initiator concentration to calculate target DP_n per arm. A ratio of $[Initiator]_{eff}$: [Copper] : Ligand] = 1 : 1 : 2 ratio used employed.

ATRP of trimethylsilyl propargyl methacrylate (8-arm star); General procedure followed using a lactose based initiator[40] under more dilute conditions (25% wt monomer) to limit the potential of star-star coupling. The initiator concentration was calculated according to eq 3 taking each bromine group as an effective initiator to calculate effective initiator concentration to calculate target DP_n per arm. A ratio of $[Initiator]_{eff}$: [Copper] : [Ligand] = 1 : 1 : 2 ratio was employed. The reaction was terminated at 49% conversion and the target DP_n based of eq 3 was

used to estimate the final DP as the lactose core protons were obscured and could not be used to determine $DP_{n,NMR}$.

General procedure for deprotection. Poly(trimethylsilyl propargyl methacrylate) (1.0 g) and acetic acid (460.0 mg, 1.5 eq mol/mol with respect to the alkyne-trimethylsilyl groups) were dissolved in THF (60 ml) and sealed. The solution was bubbled with nitrogen for 20 minutes and then cooled to -20 ^{0}C. Solution of 1 M tetrabutylammonium fluoride hydrate (5% wt water) in THF (2.3 ml, 1.5 eq mol/mol with respect to the alkyne-trimethylsilyl groups) was added slowly into the mixture via syringe. The resulting mixture was stirred at -20 ^{0}C for 30 minutes before being warmed to ambient temperature for 6 hours. The resulting mixture was passed through a short column of silica, using THF as an eluent. The resulting filtrate was concentrated under reduced pressure and the polymer was precipitated in water (150 ml). The precipitate was separated by centrifugation and decanting the water to yield poly(propargyl methacrylate) (834 mg) as white solid.

General procedure for the synthesis *N*-acetylated glycopolymers. Poly(propargyl methacrylate), sugar azide (1.2 eq mol/mol with respect to the alkyne groups), 2,2'-Bipyridine (0.2 eq mol/mol with respect to the alkyne groups) and DMSO (5ml) were charged into a dry Schlenk tube. The tube was sealed and subjected to seven freeze-pump-thaw cycles. The resulting de-gassed mixture was transferred via nitrogen under nitrogen into a second Schlenk tube, previously evacuated and filled with nitrogen, containing Cu(I)Br (1 eq mol/mol with respect to the alkyne groups) and a magnetic stirrer. The reaction mixture was stirred at room temperature for 36 hours. The glycopolymer was precipitated into THF. The precipitate was then dissolved in water and

treated with cuprisorb until the solution turned colourless. The polymer solution was then dialysed using 1KDa MWCO dialysis tubing in de-ionised water for 2 days, changing the water at least twice a day. The solution was then freeze-dried over night to yield *N*-acetylated glycopolymers as white solids.

Surface Plasmon Resonance (Amine coupling protein surface immobilisation). Sensorgrams were recording using the ProteOn XPR36 instrument (BioRad Laboratories). Lectins were immobilised on BioRad ProteOn GLC sensor chips via amine coupling at pH 5.0 using surfaces activated with sulfo-N-hydroxysuccinimide. After blocking amine coupling sites with 1 M ethanolamine pH 8.0, chip flowcells were equilibrated in running buffer (10 mM HEPES pH 7.4, 150 mM NaCl, 3 mM $CaCl_2$, 0.01 % NaN_3, 0.005 % Tween-20). Glycopolymer analytes were prepared in running buffer and flowed over the lectins at 25˚C and a flow rate of 25 µl/min. with analyte association times of 300-900 seconds.

Surface Plasmon Resonance (His-Tag Capture protein surface immobilisation). Lectins were immobilised on BioRad ProteOn HTE sensor chips via Histidine tag-capture, using 10 mM Nickel Sulfate to activate the surface. Samples were run straight after lectin immobilisation with running buffer (10 mM HEPES pH 7.4, 150 mM NaCl, 3 mM $CaCl_2$, 0.01% NaN_3, 0.005% Tween-20) at 25˚C and a flow rate of 25 µl/min for association time of 300 seconds. Running buffer was flowed immediately afterwards for dissociation phase of 375 seconds. The sensor chip was regenerated by complete removal of the lectins with 300 mM ethylene glycol-bis(β-aminoethyl ether)-*N,N,N′,N′*-tetraacetic acid (EGTA), in order to recoat the surface with new lectins.

Numerical Fit. The models (eq 1, 2) were fitted numerically using MATLAB, standard errors were gained for each parameter by confidence bound of each fit. Response at equilibrium (R_{eq}) is measured as the average response over the last 20 seconds of the association phase (response as the sensorgram curve platos). R_{max} and K_D are determined simultaneously by fitting eq 1:

$$Req = \frac{Rmax[pol]}{K_D + [Pol]} \quad \text{(eq 1)}$$

To obtain dissociation rate, a decay equation (eq 2) was fitted to the dissociation phase (buffer flow). The Response unit at the start of the dissociation phase was taken as the initial response unit (R_0):

$$R_t = R_0 \exp(-k_{off} t) \qquad \text{(eq 2)}$$

Association rate (k_{on}) was obtained from K_D and k_{off} according to the relationship (eq 4):

$$k_{on} = \frac{k_{off}}{K_D} \qquad \text{(eq 4)}$$

RESULTS AND DISCUSSION

Synthesis of the *N*-acetylated glycopolymers.

Reversible deactivation radical polymerization (RDRP) is a popular method for the preparation of glycopolymers. This study was initiated by the synthesis and polymerization of a protected alkyne-functional monomer, trimethylsilyl propargyl methacrylate (TMS-PgMA) in accordance with previous reports.[34] Atom Transfer Radical Polymerization (ATRP) of TMS-PgMA was employed using ethyl α-bromoisobutyrate (EBiB) as initiator and Cu(I)Br/*N*-(ethyl)-2-pyridylmethanimine (NEPI) as catalyst in toluene (50 wt%) at 70 ^{0}C ([TMS-PgMA] : [EBiB] : [Cu(I)Br] : [NEPI] = [80] : [1] : [1] : [2]). The polymerization was stopped before reaching full conversion to reduce

the occurrence of bimolecular termination (ρ = 68%, $DP_{n,NMR}$ = 69, $M_{n,NMR}$ = 13600 g mol^{-1}, $Đ$ = 1.30, Table 1, entry 1). Conversions were determined by monitoring the disappearance of vinylic protons at δ = 6.11 – 5.56 ppm, relative to residual $CHCl_3$ (7.26 ppm) and the degree of polymerisation (DP_n) and number average molecular weight ($M_{n,NMR}$) were determined by comparing the methylene signal present in the initiator end group (δ = 4.09 ppm) with a methylene signal in the polymer side chain at purification (δ = 4.60 ppm, Figure S1). The trimethylsilyl protecting groups were cleaved using tetra-*N*-butylammonium fluoride (TBAF) and acetic acid to afford an alkyne-functional polymer scaffold ($M_{n,NMR}$ = 8700 g mol^{-1}, $Đ$ = 1.40, Table 1, entry 2) as indicated by the disappearance of the TMS signal in ^{1}H NMR (δ = 0.2 ppm) which coincided with the appearance of a signal for the alkyne proton (δ = 2.5 ppm, Figure S2). Anomerically pure *β*-glycosyl azides of *N*-acetyl galactosamine (GalNAc) and *N*-acetyl glucosamine (GlcNAc), prepared via the one-step procedure of S. Shoda et al.[41–43] (Figure S3-6), were then 'clicked' onto the pendant alkyne groups according to a literature procedure[28] using Cu(I)Br and bypyridine to furnish GalNAc (GP1, Table 1, entry 3) and GlcNAc (GP2, Table 1, entry 4) functional glycopolymers from a single polymer scaffold. The success of the cycloaddition reaction was confirmed by FT-IR, with the disappearance of the alkyne peak (υ(C-H): 3286 cm^{-1} and υ(C≡C): 2129 cm^{-1}, Figure S7) and 1H NMR with the appearance of a signal corresponding to the triazole hydrogen (δ = 8.30 ppm, Figure S8-9).

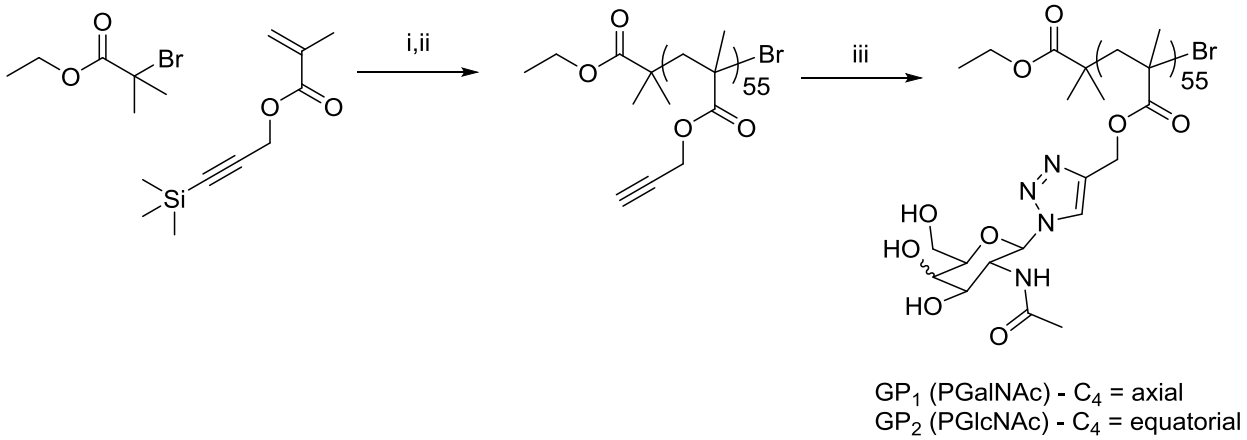

Scheme 1. Synthesis of PGalNAc prepared by sequential Cu(I)-mediated polymerization and azide-alkyne click; i) CuBr, *N*-(ethyl)-2-pyridylmethanimine, toluene, 70 °C; ii) TBAF, AcOH, THF, -20 °C; iii) CuBr, bipy, sugar azide, DMSO, RT.

Table 1. Molecular weight data for the synthesized polymer scaffold and glycopolymers

	Polymer	$M_{n,th}$ (g mol^{-1})	$M_{n,NMR}$ (g mol^{-1})	$M_{n,SEC}$[c] (g mol^{-1})	D [c]
1	P(TMSPgMA)	10900[a]	13600[b]	15400	1.30
2	P(PgMA)	6900[d]	8700[d]	9700	1.40
3	GP1	20300[d]	25600[d]	22600	1.25
4	GP2	20300[d]	25600[d]	24300	1.26

[a]Determined by $MW_{monomer}$ x conversion x $[M]_0/[I]_0$ + $MW_{initiator}$. [b]As calculated by NMR of the α-end group to determine DP_n. [c]Determined by size-exclusion chromatography (with DMF as the eluent) using conventional calibration obtained with poly(methyl methacrylate) standards (Figure S10). [d]M_n based DP_n = 69 for the P(TMSPgMA) scaffold.

Investigating binding interactions of MGL with *N*-acetylated glycopolymers (GP1-GP2).

MGL has only been reported to be expressed in subtypes of macrophages and dendritic cells as a scavenger receptor that facilitates antigen presentation of nonself-antigens.[44] MGL expression is implicated in cancer progression and binds to GalNAc based tumour-associated carbohydrate (Tn-antigen) on the mucin molecule MUC1[45] expressed by malignant cells.[46] Binding to MGL is reported to drive Th2-mediated responses via the MHC class II processing and presentation pathway,[47] as opposed to tumourcidal Th1 responses.[48] Although the engagement of MGL by ligands *per se* may not direct a specific response, it may influence and impact responses via co-engagement of other receptors.[49] Therefore, from a bottom-up approach it was necessary to investigate whether our polymers could also interact with MGL as well as closely related CTLs. The association and binding of glycopolymers to the target lectins was investigated using multi-channel Surface Plasmon Resonance (SPR).

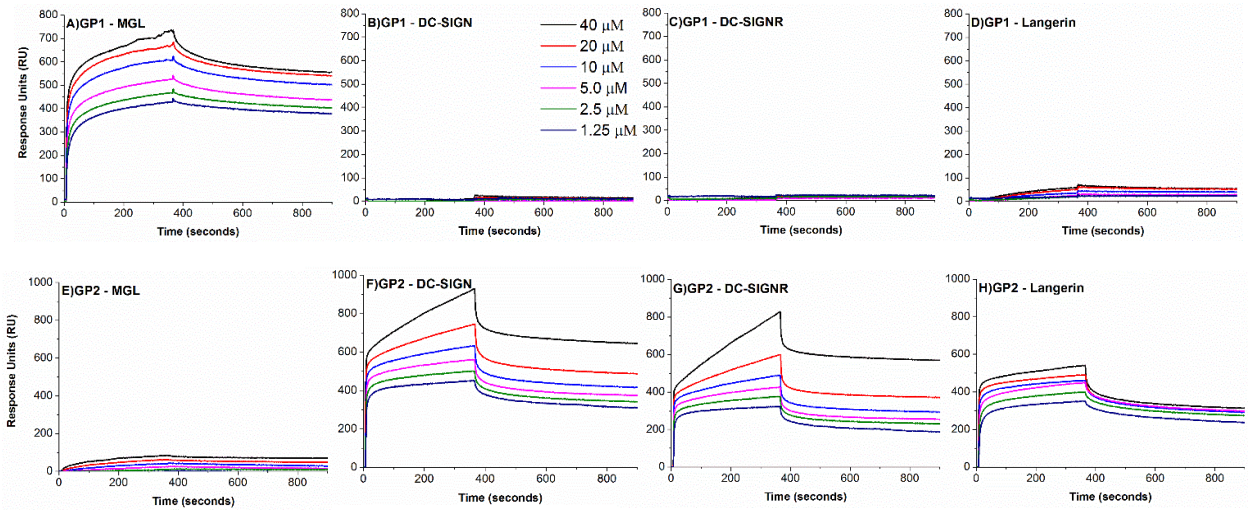

Figure 1. SPR sensorgrams for the binding of glycopolymers GP1 (A-D) and GP2 (E-H) with lectins MGL, DC-SIGN, DC-SIGNR and Langerin. GP1 / GP2 were flowed at 0.25 μLs^{-1} for 375 seconds with varying concentration range to determine association. Buffer was flowed between t = 375 and 900 seconds to establish the dissociation phase.

Soluble, recombinant MGL extracellular portion (CRD domain and coiled-coil neck) was immobilized on the chip surface through EDC-NHS mediated amine coupling with carboxylic acid coated alginate on the SPR sensor chip.[50] Extracellular portions of the closely related immunological CTLs: DC-SIGN, DC-SIGNR and Langerin were also immobilised onto chips for parallel investigations to assess their interactions with the *N*-acetylated glycopolymers **(GP1** and **GP2**). The glycopolymers (range: 1.25 – 40 μM in serial 2:1 dilution) were flowed over, in parallel, across each lectin-bearing channel, followed immediately by buffer alone (see supporting info for full details). The sensorgrams (Figure 1**)** show clear concentration dependent association of PGalNAc **GP1** to MGL with slow dissociation. **GP1** did not bind to the other lectins (DC-SIGN, DC-SIGNR and Langerin) inferring high selectivity for MGL. In contrast, PGlcNAc, **GP2** was observed to bind to DC-SIGN and other related EPN-type lectins, but did not bind to MGL **(**Figure 1, Table 2). The extent of binding can be quantified using the SPR software via a two state model for glycopolymer-lectin interactions.[26,50] From this fitting two K_D values are obtained. For the purpose of this investigation a simple Langmuir-type isotherm fitting of each interaction was employed as a parsimonious model to quantify the glycopolymer-lectin interaction as a single dissociation equilibrium constant (K_D, eq 1). Individual rate constants were obtained separately; dissociate rate (k_{off}) from the dissociation phase (eq 2) and an apparent association rate, as the quotient of K_D and k_{off}.

Table 2. Binding parameters of glycopolymers GP1 and GP2 with human lectins obtained from SPR, eq1 and eq2.

Pol	lectin	$k_{on,app}$ (x 10^2 $M^{-1}s^{-1}$)	k_{off} [b] (x 10^{-4} s^{-1})	K_D[a] (nM)

GP1	MGL	2.62	2.88	1106
	DC-SIGN	-	-	-
	DC-DIGNR	-	-	-
	Langerin	-	-	-
GP2	MGL	-	-	-
	DC-SIGN	2.49	3.59	1442
	DC-SIGNR	1.12	3.24	2907
	Langerin	8.58	4.95	577

[a] As determined by : $Req = \frac{Rmax[pol]}{K_D+[Pol]}$ (eq 1)

[b] As determined by: $R_t = R_0 \exp(-k_{off} t)$ (eq 2)

Investigating the effect of chain length and polymer architecture on binding affinity.

Typically, plant and human derived lectins exist as multimeric assemblies and as a result individual CTL-sugar interactions are weak. Multimeric, or multivalent sugar ligands often confer much stronger binding than monomeric and short oligomeric equivalents. This phenomenon is widely referred to as the 'glycoside cluster effect'.[51] One of the advantages of using RDRP protocols is the ability to control polymer chain length and architecture. Thus, it is possible to manipulate ligand multivalency by varying the number and orientation of pendant sugar groups present within target glycopolymers. Furthermore, the possibility of forming well-defined block copolymers provides access to higher-ordered structures such as micelles, vesicles and nano-gels wherein the density of sugar ligands present can in intricately controlled by the monomer feed. To this end, De Coen and coworkers have investigated the potential of mannosylated nano-gels to target MR

expressed on dendritic cells and found that increased particle size and ligand (mannose) density resulted in enhanced receptor binding and internalization.[27]

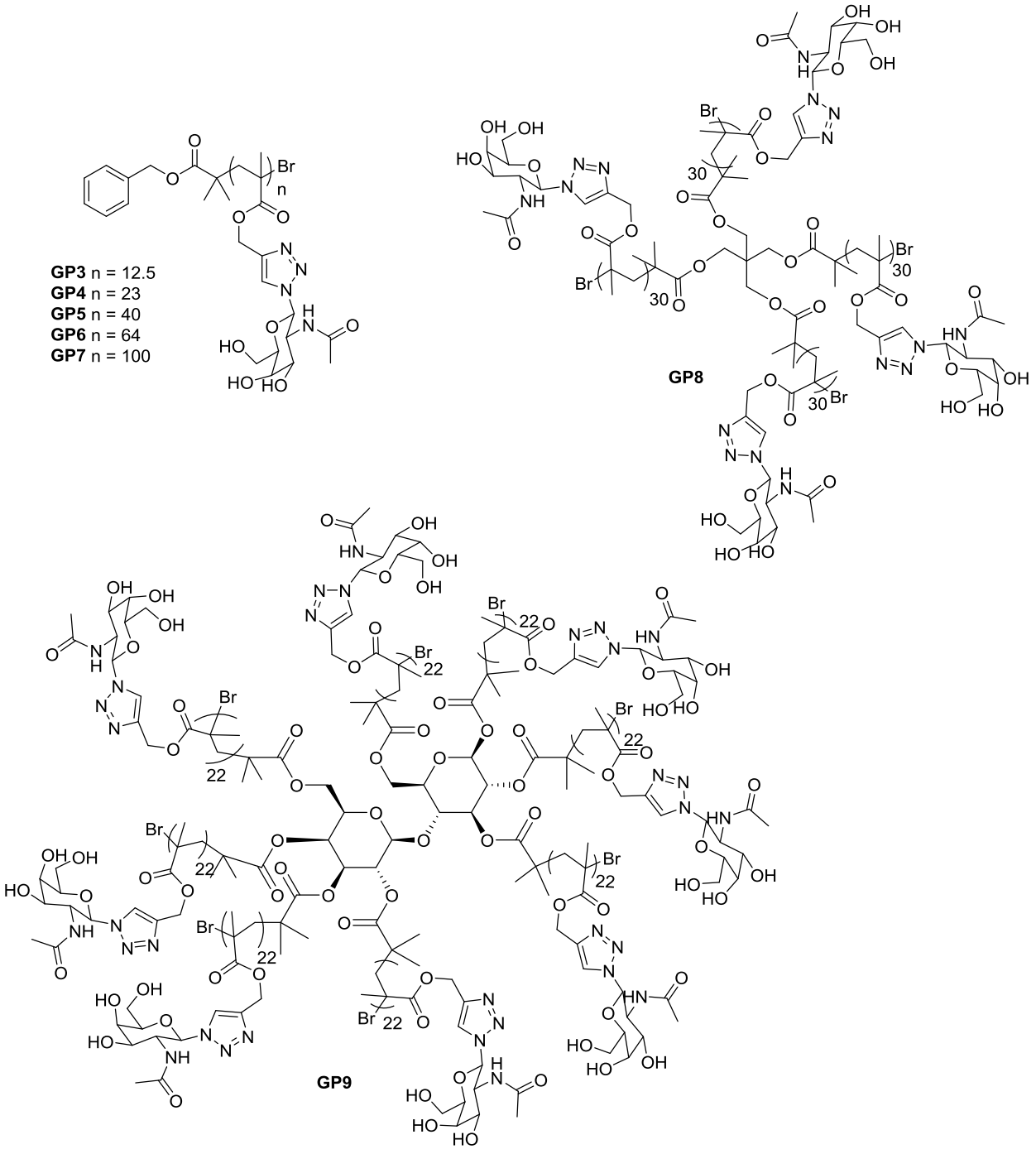

Figure 2. PGalNAc library synthesized by ATRP to investigate the effect of ligand valency on lectin binding.

To investigate the effect of polymer chain length and architecture on binding to MGL, a library of linear PGalNAc polymers (**GP3-GP7**) of varying chain length (DP_n 12-100, Table S1, Figure S11) were prepared by ATRP employing a benzyl initiator[34] which enabled more accurate analysis of the number average molecular weight by ^{1}H NMR by comparing the distinctive benzyl protons (7.28-7.38 ppm) against OCH_2-R (4.59 ppm) of the polymer side chain (Figure S12). Likewise, alternative architectures were prepared using 4-arm (pentaerythritol-based) and 8-arm (lactose-based) initiators (Figure 2). Employing ATRP, the copper and ligand concentration was adjusted to account for each initiating group. The DP_n of the 4-arm star PGalNAc (**GP8**, $M_{n,Th}$ = 45600 g.mol^{-1}, $Đ$ = 1.30, Table S1, Figure S11) was determined as 30 per arm according to the monomer conversion (ρ ~ 60 %) from an [M]:[I] ratio of 200 employed during P(TMSPgMA) scaffold synthesis. The core methylene protons (4.33 ppm) from the initiator were obscured which prohibited accurate determination of DP_n by ^{1}H NMR. Likewise the DP_n of the 8-arm star PGalNAc **(GP9,** $M_{n,Th}$ = 34900 g.mol^{-1}, $Đ$ = 1.22, Table S1, Figure S11) was also determined by monomer conversion as the core lactose ring protons (3.84 -5.86 ppm) could not be reliably integrated by ^{1}H NMR. Polymerization from the 8-arm initiator was carried out under more diluted conditions (25 wt%) with [M]:[I] ratio of 360 and was terminated at lower monomer conversion (ρ~ 49 %) to reduce the occurrence of star-star coupling,[52,53] furnishing an 8-arm star PGalNAc with DP_n of 22 per arm.

During the initial study (**GP1-2**), all lectins were covalently bound to SPR chips via established amine coupling chemistry.[26] Removal of bound polymers from covalently immobilized lectins, usually via chelation chemistry (EGTA)[54] or simple acid treatment (pH 3 glycine buffer),[26] limits

the number of sequential experiments due to denaturation of the bound proteins. For a more reliable comparison of the PGalNAc library (**GP3-9**), fresh lectin was used for each SPR experiment to ensure the binding was not influenced by the previous experiment. This was carried out using Bio-Rad Laboratories ProteOn^{TM} HTE Sensor chip, which contains *tris*-nitrilotriacetic acid, reported to have subnanomolar affinity towards His-tagged molecules.[55] Thus, His-tagged MGL was reversibly immobilized to a nickel sulfate activated SPR chip prior to analysis. Polymer-bound lectins were then rapidly removed using chelating agent EGTA before immobilization of a fresh batch of His-tagged MGL between each subsequent experiment.

The binding of PGalNAc to MGL was largely unchanged as a function of the polymer valency (Figure 3). Although increasing the linear chain length, from DP_n = 12 to DP_n = 100 (**GP3-7**) was found to lower the overall K_D of the polymer, the differences were not significant (517 – 169 nM, Figure 3, Table 3). The architecture of the PGalNAc polymers also had little effect on the binding to MGL with the 4-arm star (**GP8**) and 8-arm star PGalNAc (**GP9**), exhibiting comparable binding to the linear analogues (157 nM and 240 nM respectively, Figure 3, Table 3). A similar observation was previously reported by Stenzel and coworkers, whereby the binding of glucose-containing 4-arm star glycopolymers to ConA, did not show a significant effect on binding compared to linear analogues.[18] As the association rate directly reflects the dissociation constant by our method, a similar trend was observed whereby PGalNAc appeared to bind marginally faster as a function of increasing valency (410 – 1870 $M^{-1}.s^{-1}$, Table 3), whereas only minor changes in the dissociation rates were determined (1.66×10^{-4} s^{-1} - 3.45×10^{-4} s^{-1}, Table 3) with no obvious trend with respect to valency.

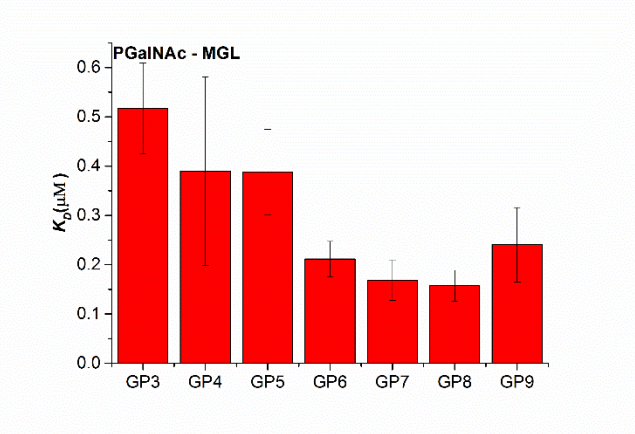

Figure 3. Binding constants of glycopolymers GP3-GP9 with MGL determined from SPR (Figure S20).

To date, the structure of MGL has not been fully elucidated, but has been reported to share similarities with DC-SIGN and Mannose binding protein (MBP) where the CRDs are relatively distant and face away from one another. Such an orientation might be expected to be ideal for cross-linking via multivalent ligands.[56] Indeed, one of the immunological functions of MGL has been attributed to cross-linking of CD45 expressed on the surface of activated T cells, modulating their behaviour.[57] Structurally, chemical cross-linking experiments have shown that MGL exists as a homotrimer.[56] Trimerization occurs in the neck domain and is independent of the CRD, with the junction between the two domains being protease sensitive. This indicates that the CRD consists of three discrete, distally orientated sugar binding sites that are potentially dynamic and capable of adjusting to compliment the glycan clusters presented to the lectin surface, similar to MBP.[56] Therefore it is proposed that the three binding sites interact independently with the PGalNAc polymers employed during this investigation. On a molecular level, this translates to the polymers not having to traverse the multiple binding sites of a single MGL trimer to enhance binding.

Relative binding of PGalNAc with ASGPR and MGL.

In comparison to MGL, ASGPR was discovered much earlier[58] and the structure and function has been more extensively explored.[59] Native human ASGPR consists of two different chains, H1 and H2, forming a hetero-oligomer.[60] Despite this, to date there are currently no crystal structures of the complete extracellular domain of the native H1/H2 heterooligomer, but the arrangement and orientation of the CRD is well investigated and optimal ASGPR ligands reported in the literature are selected based on the spatial arrangement of Gal residues within the native tri/tetra-antennary N-glycans.[61] The recombinant ASGPR used during this investigation (CRD and neck domain of H1 subunit), is a self-assembled homotrimer,[62] the structure of which closely resembles the native hetero-oligomer lectin, in which the binding sites are in close proximity,[54] presenting an interface more suitable for clustered glycosides, typically at the termini of a single, branched oligosaccharide. From previous literature pertaining to monosaccharide selectivity,[63] it was hypothesised that APSGR would exhibit similar binding selectivity to MGL. Having demonstrated binding of PGalNAc (**GP1**, 1.62 μM), and a lack of binding of PGlcNAc (**GP2**) to ASGPR (Figure 4A,B), the effect of chain length and architecture was again investigated. The overall binding of PGalNAc (**GP3-GP9**) to ASGPR was found to be lower than MGL, particularly for short polymer chain lengths (**GP3-5**, Table 3). However, a more pronounced effect on binding with changing the valency of PGalNAc was observed.

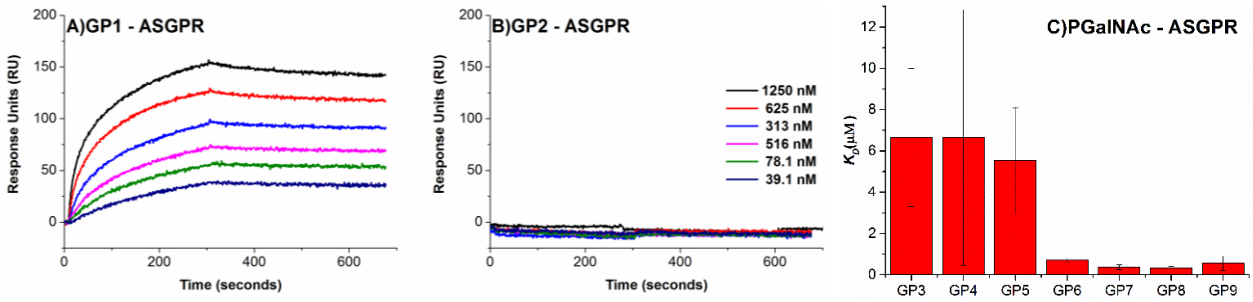

Figure 4. SPR sensorgrams for the binding of glycopolymers GP1 (A) and GP2 (B) with ASGPR. GP1 / GP2 were flowed at 0.25 µLs-1 for 300 seconds with varying concentration range to determine association. Buffer was flowed between t = 300 and 700 seconds to establish the dissociation phase. Binding constants of glycopolymers GP3-GP9 with APSGR determined from SPR (Figure S21)

Table 3. The effect of ligand valency on the binding of PGalNAc glycopolymers to MGL and ASGPR

				MGL			ASGPR		
	DP_n[a]	**M_n[a] (g.mol^{-1})**	**$Đ$[c]**	**K_D (nM)**	**$k_{on,app}$ (x 10^2 $M^{-1}.s^{-1}$)**	**k_{off} (x 10^{-4} s^{-1})**	**K_D (nM)**	**$k_{on,app}$ (x 10^2 $M^{-1}.s^{-1}$)**	**k_{off} (x 10^{-4} s^{-1})**
GP3	12	4700	1.15	**517**	4.10	2.12	**6653**	0.35	2.33
GP4	23	8800	1.34	**390**	4.27	1.66	**6652**	0.39	2.58
GP5	40	15100	1.30	**388**	8.90	3.45	**5535**	0.71	3.94
GP6	64	24000	1.13	**211**	9.17	1.94	**712**	3.56	2.57
GP7	100	37300	1.21	**169**	15.70	2.64	**372**	12.00	4.47
GP8	30 / arm[b]	45600[b]	1.30	**157**	18.70	2.94	**341**	10.20	3.47
GP9	22 / arm[b]	68000[b]	1.22	**240**	13.50	3.26	**560**	8.23	4.61

[a]Determined by ^{1}H NMR via integration of the benzyl protons (7.28-7.38 ppm) of the chain end against OC$\boldsymbol{H}_2$-R (4.59 ppm) of the polymer. [b]Approximated from data obtained for the polymer scaffold (Table S1). [c]Determined by size-exclusion chromatography (with DMF as the eluent) using conventional calibration obtained with Poly(methyl methacrylate) standards (Figure S11). [d]Determined SPR whereby GP3-9 were flowed at 0.25 µLs-1 for 375 seconds to afford association before buffer was flowed (t = 375-900 seconds) to establish the dissociation phase (Figure S20 - S21).

At shorter chain lengths, the binding of linear PGalNAc (**GP3-5**) to ASGPR was comparable (**GP3-5,** 6.7 – 5.5 μM). When the chain length was increased further, the dissociation constant decreased much more significantly than previously observed for MGL (**GP6-7,** 712 – 372 nM). Similarly to MGL, no significant effect was observed upon changing the polymer architecture (**GP8-9,** 560 - 341 nM). Molecularly, this indicates that low molecular weight PGalNAc (**GP3-5**) share similar binding modes, as indicated by minimal changes in the K_D**.** ASGPR has been reported to bind markedly weaker to monovalent GalNAc ligands and as such ASGPR ligands are often based on a tri/tetra-antennary design to compliment the more rigid, proximal binding sites of the multivalent ASGPR oligomer.[64,65] When the chain length of the PGalNAc ligand is increased beyond DP_n = 64 the binding to ASGPR is markedly enhanced as a result of the 'glycoside cluster effect' whereby the multivalent PGalNAc ligands are capable of binding to multiple binding sites of ASGPR, thus overcoming the individually weak interactions.

The differential binding of MGL and ASGPR was further exemplified using a GalNAc-BSA conjugate, where single GalNAc moieties are randomly exposed through conjugation to surface serine and threonine residues. Only binding to MGL, with its distally orientated, flexible CRD, was observed, and no binding was observed to the more rigid, proximal binding sites of ASGPR which requires more closely configured sugar ligands (Figure 5). The PGalNAc polymers synthesized during this investigation were predicted to be long enough to span the proximal binding sites of the ASGPR which are separated by approximately 15-25 Å.[66] With this in mind, the shortest PGalNAc (DP_n = 12.5, **GP3**) should be sufficiently long enough to bind to at least two of the binding sites based on a perfectly linear conformation, whilst **GP5** (DP_n = 40) should be sufficiently long enough to bind to all three binding sites of the trimer. However, the glycopolymers do not exist as ideal linear chains in solution, and as a result changes in the K_D were

only observed at longer chain lengths (**GP6-GP7,** DP_n = 64, 100). Thus, the 'glycoside cluster effect' was apparent at longer chain lengths as the conformation of the polymer in solution promotes binding at multiple sites of the lectin CRD. Furthermore, beyond a critical chain length, secondary interactions that result in cross-linking between ASGPR oligomers are possible which could contribute to the stronger binding interactions observed.

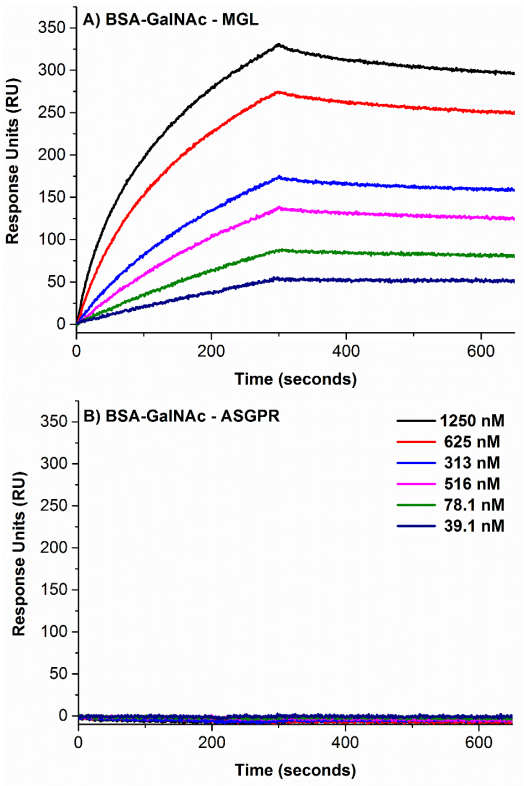

Figure 5. SPR sensorgrams for the binding of BSA-GalNAc conjugate to MGL (A) and ASGPR (B). BSA-GalNAc conjugate was flowed at 0.25 µLs-1 for 300 seconds with varying concentration range to determine association. Buffer was flowed between t = 300 and 700 seconds to establish the dissociation phase.

Bertozzi *et al.* previously described an analogous system in plant lectins; Helix Pomatia Agglutinin (HPA) and Soybean Agglutinin (SBA), where HPA (proximal binding sites) was found to interact strongly in a valence independent manner and SBA (distant binding sites) to reversibly 'bind and

slide' leading weaker interactions.[19] Conversely, this investigation has demonstrated that binding to ASGPR, with proximal binding sites, occurs in a valence dependent manner, whereas MGL, with its flexible, distal binding sites binds independent of valence with affinity attributed a preference for multi-molecular lectin binding via cross-linking through the glycopolymer scaffold. These contrasting conclusions serve to highlight the complexity of lectin/glycopolymer interactions which are strongly dependent upon the nature of lectin(s) and polymers under investigation.

CONCLUSION

A library of PGalNAc glycopolymers have been used for the first time to perform binding studies with human CTL's MGL and ASGPR. A polyalkyne scaffold prepared by Cu(I)-mediated radical polymerization was functionalized with azido-GalNAc and azido-GlcNAc respectively and the binding and selectivity of the resulting polymers was assessed against target lectins MGL and ASGPR as well as related CTLs DC-SIGN, DC-SIGNR and Langerin using SPR. PGalNAc was found to specifically bind to MGL and shows little affinity for related CTLs. Conversely, PGlcNAc exhibits little affinity for MGL but binds to the related CTLs with varying affinity. Increasing the ligand valency by increasing the DP_n of the PGalNAc resulted in only a small increase in affinity, which remained unchanged as a function of polymer architecture. This is attributed to the distal orientation and flexibility of the carbohydrate binding domain of MGL. One the other hand ASGPR, which is known to have a more proximal orientated binding domain, exhibits comparable selectivity of PGalNAc and conforms in-part, to the 'glycoside cluster effect.' For example, increasing the GalNAc valency by increasing the DP_n of the PGalNAc exhibited a marked increase in affinity. The specific binding thresholds reported are opportunistic for further exploitation, with potential implications in tissue-selective drug delivery. For example, it is known that GalNAc

based ligands can successfully target the liver via ASGPR *in vivo* without being obstructed by the immune system.[67] Therefore, ASGPR represents a promising entry for liver-specific drug and gene delivery using PGalNAc glycopolymers. Alternatively, selectively targeting the immune system using GalNAc based systems represents a greater challenge due to competitive uptake by the hepatic system. It is hoped that the differential binding observed between MGL and ASGPR in this study can be exploited to systemically target macrophages and DCs via MGL without off-target uptake to liver via ASGPR. Due to their pivotal role in tumour immunology, macrophages and DCs could provide a set of clinically valuable targets.[68] Thus targeting tumour environments via the carbohydrate binding properties of MGL could provide a favourable and selective therapeutic delivery strategy, due to its higher expression in sites of solid tumours.[69]

ASSOCIATED CONTENT

This material is available free of charge via the Internet at http://pubs.acs.org. This includes representative spectra of the sugar azides and glyocpolymers synthesized as well the SPR sensograms obtained.

AUTHOR INFORMATION

Corresponding Author

*p.wilson.1@warwick.ac.uk

*d.mitchell@warwick.ac.uk

Present Addresses

† Nanjing University of Science and Technology, School of Environmental and Biological Engineering, Nanjing University, Luohan Alley, Xuanwu Qu, Nanjing Shi, Jiangsu Sheng, China, 210094.

ACKNOWLEDGMENT

The authors gratefully acknowledge financial support from Engineering and Physical Sciences Research Council (EPSRC) under grant EP/F500378/1 through the Molecular Organisation and Assembly in Cells Doctoral Training Centre (MOAC-DTC). The authors also wish to acknowledge the facilities and personnel (K.K., D.M.H., T.P.D., S.P., P.W.) enabled by the Monash-Warwick Alliance. This work was carried out in conjunction with the Australian Research Council (ARC) Centre of Excellence in Convergent Bio-NanoScience and Technology (CE140100036). A.S.M. holds a Medical Research Award from the General Charity of the City of Coventry. R.W. is funded by Syngenta. K.K. gratefully acknowledges the award of a NHMRC-ARC Dementia Research Development Fellowship (APP1109945). T.P.D. gratefully acknowledges support from the ARC in the form of an Australian Laureate Fellowship. S.P. acknowledges a Royal Society Wolfson Merit Award (WM130055). PW thanks the Leverhulme Trust for the award of an Early Career Fellowship (ECF/2015-075).

REFERENCES

(1) Zanetta, J.-P.; Kuchler, S.; Maschke, S.; Thomas, D.; Dufourcq, P.; Vincendon, G. *Histochem. J.* **1992**, *24*, 791–804.

(2) Glavey, S. V; Huynh, D.; Reagan, M. R.; Manier, S.; Moschetta, M.; Kawano, Y.; Roccaro, A. M.; Ghobrial, I. M.; Joshi, L.; Dwyer, M. E. O. *Blood Rev.* **2015**, *29*, 269–279.

(3) Kooyk, Y. Van; Ilarregui, J. M.; Vliet, S. J. Van. *Immunobiology* **2015**, *220*, 185–192.

(4) Liu, F.; Patterson, R. J.; Wang, J. L. *Biochim. Biophys. Acta* **2002**, *1572*, 263–273.

(5) Urban, Š.; Anderluh, M. *Cell. Signal.* **2010**, *22*, 1397–1405.

(6) Zachara, N. E.; Hart, G. W. *Biochim. Biophys. Acta* **2006**, *1761*, 599–617.

(7) Spiess, M. *Biochemistry* **1990**, *29*, 10009–10018.

(8) Ohta, M.; Ishida, A.; Toda, M.; Akita, K.; Inoue, M.; Yamashita, K. *Biochem. Biophys. Res. Commun.* **2010**, *402*, 663–669.

(9) Sunasee, R.; Narain, R. *Macromol. Biosci.* **2013**, *13*, 9–27.

(10) Lee, R. T.; Hsu, T. L.; Huang, S. K.; Hsieh, S. L.; Wong, C. H.; Lee, Y. C. *Glycobiology* **2011**, *21*, 512–520.

(11) Cambi, A.; Koopman, M.; Figdor, C. G. *Cell. Microbiol.* **2005**, *7*, 481–488.

(12) Kolatkar, A. R.; Weis, W. I. *J. Biol. Chem.* **1996**, *271*, 6679–6685.

(13) Grozovsky, R.; Begonja, A. J.; Liu, K.; Visner, G.; Hartwig, J. H.; Falet, H.; Hoffmeister, K. M. *Nat. Med.* **2014**, *21*, 47–54.

(14) Hoffmeister, K. M. *J. Thromb. Haemost.* **2011**, *9*, 35–43.

(15) Richards, S.-J.; Otten, L.; Gibson, M. I. *J. Mater. Chem. B* **2016**, *4*, 3046–3053.

(16) Song, E.; Manganiello, M. J.; Chow, Y.; Ghosn, B.; Convertine, A. J.; Stayton, P. S.; Schnapp, L. M.; Ratner, D. M. *Biomaterials* **2012**, *33*, 6889–6897.

(17) Hayward, A. S.; Eissa, A. M.; Maltman, D. J.; Sano, N.; Przyborski, S. A.; Cameron, N. R. *Biomacromolecules* **2013**, *14*, 4271–4277.

(18) Chen, Y.; Chen, G.; Stenzel, M. H. *Macromolecules* **2010**, *43*, 8109–8114.

(19) Godula, K.; Bertozzi, C. R. *J. Am. Chem. Soc.* **2012**, *134*, 15732–15742.

(20) Lu, J.; Zhang, W.; Richards, S.-J.; Gibson, M. I.; Chen, G. *Polym. Chem.* **2014**, *5*, 2326–

2332.

(21) Godula, K.; Bertozzi, C. R. *J. Am. Chem. Soc.* **2010**, *132*, 9963–9965.

(22) Albertin, L.; Stenzel, M. H.; Barner-Kowollik, C.; Foster, L. J. R.; Davis, T. P. *Macromolecules* **2005**, *38*, 9075–9084.

(23) Albertin, L.; Kohlert, C.; Stenzel, M.; Foster, J. R.; Davis, T. P. *Biomacromolecules* **2004**, *5*, 255–260.

(24) Parry, A. L.; Clemson, N. a; Ellis, J.; Bernhard, S. S. R.; Davis, B. G.; Cameron, N. R. *J. Am. Chem. Soc.* **2013**, *135*, 9362–9365.

(25) Zhang, Q.; Wilson, P.; Anastasaki, A.; McHale, R.; Haddleton, D. M. *ACS Macro Lett.* **2014**, *3*, 491–495.

(26) Zhang, Q.; Collins, J.; Anastasaki, A.; Wallis, R.; Mitchell, D. A.; Becer, C. R.; Haddleton, D. M. *Angew. Chemie Int. ed* **2013**, *52*, 4435–4439.

(27) De Coen, R.; Vanparijs, N.; Risseeuw, M. D. P.; Lybaert, L.; Louage, B.; De Koker, S.; Kumar, V.; Grooten, J.; Taylor, L.; Ayres, N.; Van Calenbergh, S.; Nuhn, L.; De Geest, B. G. *Biomacromolecules* **2016**, *17*, 2479–2488.

(28) Zhang, Q.; Anastasaki, A.; Li, G.-Z.; Haddleton, A. J.; Wilson, P.; Haddleton, D. M. *Polym. Chem.* **2014**, *5*, 3876.

(29) Basuki, J. S.; Esser, L.; Duong, H. T. T.; Zhang, Q.; Wilson, P.; Whittaker, M. R.; Haddleton, D. M.; Boyer, C.; Davis, T. P. *Chem. Sci.* **2014**, *5*, 715.

(30) Das, A.; Theato, P. *Chem. Rev.* **2016**, *116*, 1434–1495.

(31) Slavin, S.; Burns, J.; Haddleton, D. M.; Becer, C. R. *Eur. Polym. J.* **2011**, *47*, 435–446.

(32) Krieg, A.; Becer, C. R.; Hoogenboom, R.; Schubert, U. S. *Macromol. Symp.* **2009**, *275–276*, 73–81.

(33) Semsarilar, M.; Ladmiral, V.; Perrier, S. *Macromolecules* **2010**, *43*, 1438–1443.

(34) Ladmiral, V.; Mantovani, G.; Clarkson, G. J.; Cauet, S.; Irwin, J. L.; Haddleton, D. M.; Jean, F.; Valery, F. *J. Am. Chem. Soc.* **2006**, *19*, 4823–4830.

(35) Nurmi, L.; Lindqvist, J.; Randev, R.; Haddleton, D. M. *Chem. Commun.* **2009**, 2727–2729.

(36) Haddleton, D. M.; Crossman, M. C.; Dana, B. H.; Duncalf, D. J.; Heming, A. M.; Kukulj, D.; Shooter, A. J. *Macromolecules* **1999**, *32*, 2110–2119.

(37) Mitchell, D. A.; Fadden, A. J.; Drickamer, K. *J. Biol. Chem.* **2001**, *276*, 28939–28945.

(38) Hong, S. Y.; Tobias, G.; Oualid, F. El; Errey, J. C.; Doores, K. J.; Kirkland, A. I.; Nellist, P. D.; Green, M. L. H.; Davis, B. G.; Ballesteros, B.; El Oualid, F.; Errey, J. C.; Doores, K. J.; Kirkland, A. I.; Nellist, P. D.; Green, M. L. H.; Davis, B. G.; Oualid, F. El; Errey, J. C.; Katie, J. *J. Am. Chem. Soc.* **2007**, *129*, 10966–10967.

(39) Jones, M.-C.; Ranger, M.; Leroux, J.-C. *Bioconjug. Chem.* **2003**, *14*, 774–781.

(40) Limer, A. J.; Rullay, A. K.; San, V.; Peinado, C.; Keely, S.; Fitzpatrick, E.; Carrington, S. D.; Brayden, D.; Haddleton, D. M. *React. Funct. Polym.* **2006**, *66*, 51–64.

(41) Vinson, N.; Gou, Y.; Becer, C. R.; Haddleton, D. M.; Gibson, M. I. *Polym. Chem.* **2011**, *2*, 107.

(42) Tanaka, T.; Ishitani, H.; Miura, Y.; Oishi, K.; Takahashi, T.; Suzuki, T.; Shoda, S. I.; Kimura, Y. *ACS Macro Lett.* **2014**, *3*, 1074–1078.

(43) Shoda, S.-I.; Tanaka, T.; Nagai, H.; Noguchi, M.; Kobayashi, A. *Chem. Commun.* **2009**, 3378–3379.

(44) Napoletano, C.; Zizzari, I. G.; Rughetti, A.; Rahimi, H.; Irimura, T.; Clausen, H.; Wandall, H. H.; Belleudi, F.; Bellati, F.; Pierelli, L.; Frati, L.; Nuti, M. *Eur. J. Immunol.* **2012**, *42*, 936–945.

(45) Saeland, E.; Van Vliet, S. J.; Bäckström, M.; Van Den Berg, V. C. M.; Geijtenbeek, T. B. H.; Meijer, G. a.; Van Kooyk, Y. *Cancer Immunol. Immunother.* **2007**, *56*, 1225–1236.

(46) Hollingsworth, M. a.; Swanson, B. J. *Nat. Rev. Cancer* **2004**, *4*, 45–60.

(47) Napoletano, C.; Rughetti, A.; Agervig Tarp, M. P.; Coleman, J.; Bennett, E. P.; Picco, G.; Sale, P.; Denda-Nagai, K.; Irimura, T.; Mandel, U.; Clausen, H.; Frati, L.; Taylor-Papadimitriou, J.; Burchell, J.; Nuti, M. *Cancer Res.* **2007**, *67*, 8358–8367.

(48) Carlos, C. a.; Dong, H. F.; Howard, O. M. Z.; Oppenheim, J. J.; Hanisch, F.-G.; Finn, O. J. *J. Immunol.* **2005**, *175*, 1628–1635.

(49) Zizzari, I. G.; Napoletano, C.; Battisti, F.; Rahimi, H.; Caponnetto, S.; Pierelli, L.; Nuti, M.; Rughetti, A. *J. Immunol. Res.* **2015**, *2015*, 8 pages.

(50) Becer, C. R.; Gibson, M. I.; Geng, J.; Ilyas, R.; Wallis, R.; Mitchell, D. a.; Haddleton, D. M. *J. Am. Chem. Soc.* **2010**, *132*, 15130–15132.

(51) Lundquist, J. J.; Toone, E. J. *Chem. Rev.* **2002**, *102*, 555–578.

(52) Barner-Kowollik, C.; Davis, T. P.; Stenzel, M. H. *Aust. J. Chem.* **2006**, *59*, 719–727.

(53) Whitfield, R.; Anastasaki, A.; Truong, N. P.; Wilson, P.; Kempe, K.; Burns, J. A.; Davis, T. P.; Haddleton, D. M. *Macromolecules* **2016**, *49*, 8914–8924.

(54) Venkatraman Girija, U.; Furze, C. M.; Gingras, A. R.; Yoshizaki, T.; Ohtani, K.; Marshall, J. E.; Wallis, a K.; Schwaeble, W. J.; El-Mezgueldi, M.; Mitchell, D. a; Moody, P. C. E.; Wakamiya, N.; Wallis, R. *BMC Biol.* **2015**, *13*, 27.

(55) Huang, Z.; Hwang, P.; Watson, D. S.; Cao, L.; Szoka, F. C. *Bioconjug. Chem.* **2009**, *20*, 1667–1672.

(56) Jégouzo, S. A.; Quintero-Martínez, A.; Ouyang, X.; Dos Santos, Á.; Taylor, M. E.; Drickamer, K. *Glycobiology* **2013**, *23*, 853–864.

(57) van Vliet, S. J.; Gringhuis, S. I.; Geijtenbeek, T. B. H.; van Kooyk, Y. *Nat. Immunol.* **2006**, *7*, 1200–1208.

(58) Ashwell, G.; Morell, A. G. *Adv. Enzym. Relat. Areas Mol. Biol.* **1974**, *41*, 99–128.

(59) Weigel, P. H.; Yik, J. H. N. *Biochim. Biophys. Acta* **2002**, *1572*, 341–363.

(60) Bischoff, J.; Lodish, H. F. *J. Biol. Chem.* **1987**, *262*, 11825–11832.

(61) Khorev, O.; Stokmaier, D.; Schwardt, O.; Cutting, B.; Ernst, B. *Bioorganic Med. Chem.* **2008**, *16*, 5216–5231.

(62) Geffen, I.; Wessels, H. P.; Roth, J.; Shia, M. a; Spiess, M. *Embo J.* **1989**, *8*, 2855–2861.

(63) van Vliet, S. J.; Liempt, E. van; Saeland, E.; Aarnoudse, C. A.; Appelmelk, B.; Irimura, T.; Geijtenbeek, T. B. H.; Blixt, O.; Alvarez, R.; Die, I. van; Kooyk, Y. Van. *Int. Immunol.* **2005**, *17*, 661–669.

(64) Biessen, E. A. L.; Beuting, D. M.; Roelen, H. C. P. F.; Boom, J. H. Van; Berkelf, T. J. C. Van. *J. Med. Chem.* **1995**, *38*, 1538–1546.

(65) Prakash, T. P.; Yu, J.; Migawa, M. T.; Kinberger, G. A.; Wan, W. B.; Østergaard, M. E.; Carty, R. L.; Vasquez, G.; Low, A.; Chappell, A.; Schmidt, K.; Aghajan, M.; Crosby, J.; Murray, H. M.; Booten, S. L.; Hsiao, J.; Soriano, A.; Machemer, T.; Cauntay, P.; Burel, S. A.; Murray, S. F.; Gaus, H.; Graham, M. J.; Swayze, E. E.; Seth, P. P. *J. Med. Chem.* **2016**, *59*, 2718–2733.

(66) Meier, M.; Bider, M. D.; Malashkevich, V. N.; Spiess, M.; Burkhard, P. *J. Mol. Biol.* **2000**, *300*, 857–865.

(67) Dhande, Y. K.; Wagh, B. S.; Hall, B. C.; Sprouse, D.; Hackett, P. B.; Reineke, T. M. *Biomacromolecules* **2016**, Articles ASAP.

(68) Solinas, G.; Schiarea, S.; Liguori, M.; Fabbri, M.; Pesce, S.; Zammataro, L.; Pasqualini, F.; Nebuloni, M.; Chiabrando, C.; Mantovani, a.; Allavena, P. *J. Immunol.* **2010**, *185*, 642–652.

(69) Allavena, P.; Chieppa, M.; Bianchi, G.; Solinas, G.; Fabbri, M.; Laskarin, G.; Mantovani, A. *Clin. Dev. Immunol.* **2010**, *2010*, 547179.

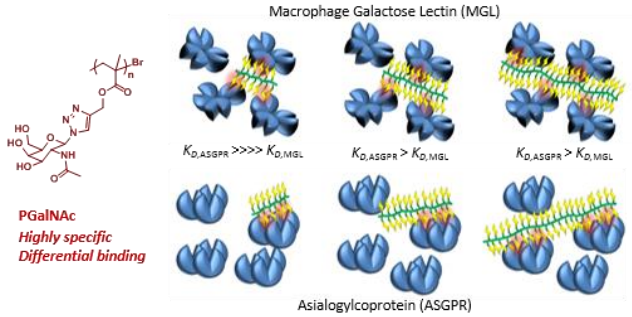
Macrophage Galactose Lectin (MGL)
$K_{D,ASGPR}$ >>>> $K_{D,MGL}$
$K_{D,ASGPR}$ > $K_{D,MGL}$
$K_{D,ASGPR}$ > $K_{D,MGL}$
PGalNAc
Highly specific
Differential binding
Asialogylcoprotein (ASGPR)